High-Precision Determination of the $Z - Z'$ Mixing Angle at LHC

A.A. Pankov*, A.V. Tsytrinov†

Abdus Salam ICTP Affiliated Centre
at Sukhoi State Technical University of Gomel

Abstract

We consider the expected sensitivity to Z' boson effects in the $W^{\pm}$ boson pair production process at the Large Hadron Collider (LHC). The results of a model-dependent analysis of Z' boson effects are presented as constraints on the Z-Z' mixing angle ϕ and Z' boson mass. We show that the process $pp \to W^+W^- + X$ allows to place stringent constraints on the Z-Z' mixing angle.

1 Introduction

Many New Physics (NP) scenarios beyond the Standard Model (SM) [1], including superstring and left-right-symmetric models, predict the existence of new neutral gauge bosons, which might be light enough to be accessible at current and/or future colliders [2–5].

The search for these Z' particles is an important aspect of the experimental physics program of current and future high-energy colliders. Present limits from direct production at the LHC and virtual effects at LEP, through interference or mixing with the Z boson, imply that new Z' bosons are rather heavy and mix very little with the Z boson. Depending on the considered theoretical model, Z' masses of the order of 2.5–3.0 TeV [6–9] and Z-Z' mixing angles at the level of a few per mil are excluded [10–12]. The size of the mixing angle is strongly constrained by

*E-mail:pankov@ictp.it
†E-mail:tsytrin@rambler.ru

very high precision Z-pole experiments at LEP and the SLC [13]. They contain measurements from the Z line shape, from the leptonic branching ratios normalized to the total hadronic Z decay width and from leptonic forward-backward asymmetries. A Z' boson, if lighter than about 5 TeV, could be discovered at the LHC [14,15] with $\sqrt{s} = 14$ TeV in the Drell-Yan process

$$pp \to Z' \to \ell^+\ell^- + X \tag{1}$$

with $\ell = e, \mu$. The future e^+e^- International linear collider (ILC) with high c.m. energies and longitudinally polarized beams could indicate the existence of Z' bosons via its interference effects in fermion pair production processes, with masses up to about $6 \times \sqrt{s}$ [16] while Z-Z' mixing will be constrained down to $\sim 10^{-4} - 10^{-3}$ in the process $e^+e^- \to W^+W^-$ [17,18].

After the discovery of a Z' boson at the LHC via the process (1), some diagnostics of its couplings and Z-Z' mixing needs to be done in order to identify the correct theoretical framework. In this paper we study the potential of the LHC to discover Z-Z' mixing effects in the process

$$pp \to W^+W^- + X \tag{2}$$

and compare it with that expected at the ILC.

The $W^\pm$ boson pair production process (2) is rather important for studying the electroweak gauge symmetry at the LHC. Properties of the weak gauge bosons are closely related to electroweak symmetry breaking and the structure of the gauge sector in general. In addition, the diboson decay modes of Z' directly probe the gauge coupling strength between the new and the standard-model gauge bosons. The coupling strength strongly influences the decay branching ratios and the natural widths of the new gauge bosons. Thus, detailed examination of the process (2) will both test the gauge sector of the SM with the highest accuracy and throw light on NP that may appear beyond the SM.

Direct searches for a heavy WW resonance have been performed by the CDF and D0 collaborations at the Tevatron. The D0 collaboration explored diboson resonant production using the $\ell\nu\ell'\nu'$ and $\ell\nu jj$ final states [19]. The CDF collaboration also searched for resonant WW production in the $e\nu jj$ final state, resulting in a lower limit on the mass of an RS graviton, Z' and W' bosons [12].

The direct WW resonance search by the ATLAS Collaboration using $l\nu l'\nu'$ final-state events in 4.7 fb^{-1} pp collision data at the collider energy of 7 TeV set mass limits on such resonances [20, 21]. Also, the $l\nu jj$ final state allows to reconstruct the invariant mass of the system, under certain assumptions on the neutrino momentum from a W boson decay.

Here, we examine the feasibility of observing a Z' boson in the $W^\pm$ pair production process at the LHC, which in contrast to the Drell-Yan process (1) is not the principal discovery channel, but can help to understand the origin of new gauge bosons.

2 Z' models

There are many theoretical models which predict a Z' with mass possibly in the TeV range. Popular classes of models are represented by E_6-motivated models, the Left-Right Symmetric Model (LR), the Z' in an 'alternative' left-right scenario and the Sequential Standard Model (SSM), which has a heavier boson with couplings like those of the SM Z. Searching for Z' in the above models has been widely studied in the literature [2–4] and applied at LEP2, the Tevatron and the LHC. For the notation we refer to [17], where also a brief description can be found. The different models considered are: (i) Models related to the breaking of E_6, parametrized by a parameter β, familiar cases are the Z'_χ, Z'_ψ, Z'_η and Z'_I models; (ii) Left-right models, originating from the breaking down of an $SO(10)$ grand-unification symmetry, leading to a $Z'_{\rm LR}$; (iii) The sequential $Z'_{\rm SSM}$, which has couplings to fermions being the same as those of the SM Z.

The mass-squared matrix of the Z and Z' can have non-diagonal entries δM^2, which are related to the vacuum expectation values of the fields of an extended Higgs sector:

$$M^2_{ZZ'} = \begin{pmatrix} M_Z^2 & \delta M^2 \\ \delta M^2 & M_{Z'}^2 \end{pmatrix} . \tag{3}$$

Here, Z and Z' denote the weak gauge boson eigenstates of $SU(2)_L \times U(1)_Y$ and of the extra $U(1)'$, respectively. The mass eigenstates, Z_1 and Z_2, diagonalizing the matrix (3), are then obtained by the rotation of the fields Z and Z':

$$Z_1 = Z\cos\phi + Z'\sin\phi\ , \tag{4a}$$

$$Z_2 = -Z\sin\phi + Z'\cos\phi\ . \tag{4b}$$

Here, the mixing angle ϕ is expressed in terms of masses as:

$$\tan^2\phi = \frac{M_Z^2 - M_1^2}{M_2^2 - M_Z^2} \simeq \frac{2M_Z\Delta M}{M_2^2}\ , \tag{5}$$

where $\Delta M = M_Z - M_1 > 0$, M_Z being the mass of the Z_1 boson in the absence of mixing, i.e., for $\phi = 0$. Once we assume the mass M_1 to be determined experimentally, the mixing depends on two free parameters, which we identify as ϕ and M_2.

From (4), one obtains the vector and axial-vector couplings of the Z_1 and Z_2 bosons to fermions:

$$v_{1f} = v_f \cos\phi + v'_f \sin\phi \ , \ a_{1f} = a_f \cos\phi + a'_f \sin\phi \ , \tag{6a}$$

$$v_{2f} = v'_f \cos\phi - v_f \sin\phi \ , \ a_{2f} = a'_f \cos\phi - a_f \sin\phi \ , \tag{6b}$$

with $(v_f, a_f) = (g_L^f \pm g_R^f)/2$, and (v'_f, a'_f) similarly defined in terms of the Z' couplings. The fermionic Z' couplings can be found, e.g. in [17].

Analogously, one obtains according to the remarks above:

$$g_{WWZ_1} = \cos\phi \, g_{WWZ} \ , \tag{7a}$$

$$g_{WWZ_2} = -\sin\phi \, g_{WWZ} \ , \tag{7b}$$

where $g_{WWZ} = \cot\theta_W$.

3 Cross section

The parton model cross section for the process (2) from initial quark-antiquark states can be written as

$$\frac{d\sigma_{q\bar{q}}}{dM\,dy\,dz} = K\frac{2M}{s}\sum_q [f_{q|P_1}(\xi_1)f_{\bar{q}|P_2}(\xi_2) + f_{\bar{q}|P_1}(\xi_1)f_{q|P_2}(\xi_2)]\,\frac{d\hat{\sigma}_{q\bar{q}}}{dz} \ . \tag{8}$$

Here, s is the proton-proton center-of-mass energy squared; $z = \cos\theta$ with θ the W^--boson–quark angle in the W^+W^- center-of-mass frame; y is the diboson rapidity; $f_{q|P_1}(\xi_1, M)$ and $f_{\bar{q}|P_2}(\xi_2, M)$ are parton distribution functions in the protons P_1 and P_2, respectively, with $\xi_{1,2} = (M/\sqrt{s})\exp(\pm y)$ the parton fractional momenta; finally, $d\hat{\sigma}_{q\bar{q}}/dz$ are the partonic differential cross sections. In (8), the K factor accounts for next-to-leading order QCD contributions [22,23]. For simplicity, we will use as an approximation a global flat value $K = 1.2$ [24, 25] both for the SM and Z' boson cases. For numerical computation, we use CTEQ-6L1 parton distributions [26]. Since our estimates will be at the Born level, the factorisation scale $\mu_{\rm F}$ enters solely through the parton distribution functions, as the parton-level cross section at this order does not depend on $\mu_{\rm F}$. As regards the scale dependence of the parton distributions we choose for the factorization scale the WW invariant mass, i.e., $\mu_{\rm F}^2 = M^2 = \hat{s}$, with $\hat{s} = \xi_1\,\xi_2\,s$ the parton subprocess c.m. energy squared. We have checked that the obtained constraints presented in the following are not significantly modified when $\mu_{\rm F}$ is varied in the interval $\mu_{\rm F}/2$ to $2\mu_{\rm F}$.

Taking into account the experimental rapidity cut relevant to the LHC experiments, ($Y_{\rm cut} = 2.5$), one should carry out the integration over the phase space in (8) determined as [27, 28]:

$$|y| \leq Y = \min\left[\ln(\sqrt{s}/M), Y_{\rm cut}\right] = \ln(\sqrt{s}/M), \tag{9}$$

where we do not consider low masses, $\ln(\sqrt{s}/M) < Y_{\rm cut}$. This leads to a cut in the production angle

$$|z| \leq z_{\rm cut} = \min\left[\tanh(Y_{\rm cut} - |y|)/\beta_W, 1\right] \ , \tag{10}$$

where $\beta_W = \sqrt{1 - 4M_W^2/\hat{s}}$ and M_W is the W boson mass.

The resonant Z' production cross section of process (2) needed in order to estimate the expected number of Z' events, can be derived from (8) by integrating its right-hand-side over z, the rapidity of the $W^\pm$-pair y and invariant mass M around the resonance peak ($M_R - \Delta M/2$, $M_R + \Delta M/2$):

$$\sigma(pp \to W^+W^- + X) = \int_{M_R-\Delta M/2}^{M_R+\Delta M/2} dM \int_{-Y}^{Y} dy \int_{-z_{\rm cut}}^{z_{\rm cut}} dz \frac{d\sigma_{q\bar{q}}}{dM\, dy\, dz} \ . \tag{11}$$

We adopt the parametrization of the experimental mass resolution ΔM in reconstructing the diboson invariant mass of the W^+W^- system, ΔM vs. M, as proposed in Ref. [29]. (After integration over y, interference effects vanish.)

The parton level $W^\pm$ boson pair production can be described, within the gauge models discussed here, by the subprocesses

$$q\bar{q} \to \gamma, Z_1, Z_2 \to W^+W^-, \tag{12}$$

as well as t- and u-channel amplitudes.

The differential (unpolarized) cross section of process (12) can be written as:

$$\frac{d\hat{\sigma}_{q\bar{q}}}{dz} = \frac{1}{N_C}\,\frac{\beta_W}{32\pi\hat{s}} \sum_{\lambda,\lambda',\tau,\tau'} |F_{\lambda\lambda'\tau\tau'}(\hat{s},\theta)|^2 \ . \tag{13}$$

Here, N_C is the number of quark colors; $\lambda = -\lambda' = \pm 1/2$ are the quark helicities; the helicities of the W^- and W^+ are denoted by $\tau, \tau' = \pm 1, 0$. The helicity amplitudes $F_{\lambda\lambda'\tau\tau'}(\hat{s}, \theta)$ are summarized in Ref. [27]. There $\hat{s}$, $\hat{t}$, $\hat{u}$ are the Mandelstam variables defined as $\hat{t} = M_W^2 - \hat{s}(1-\beta_W z)/2$, $\hat{u} = M_W^2 - \hat{s}(1+\beta_W z)/2$; $\Gamma_{1,2}$ are $Z_{1,2}$ boson decay widths; $g_{1,f}^{\lambda} = v_{1,f} - 2a_{1,f}\lambda$, $g_{2,f}^{\lambda} = v_{2,f} - 2a_{2,f}\lambda$; and $\gamma_W = \sqrt{\hat{s}}/2M_W$. In the t- and u-channel exchanges we account for the initial $q = u, d, s, c$, only the CKM favoured quarks in the approximation of unity relevant matrix element.

In evaluation of the total width Γ_2 of the Z_2 boson we take into account its decay channels into fermions and $W^{\pm}$ boson pair [30]:

$$\Gamma_2 = \sum_f \Gamma_2^{ff} + \Gamma_2^{WW} \ . \tag{14}$$

Further contributions of decays involving Higgs and/or gauge bosons and supersymmetric partners (including sfermions), which are not accounted for in (14), could increase Γ_2 by a model-dependent amount typically as large as 50% [30]. For definiteness the Z_2 width Γ_2 is assumed to scale with the Z_2 mass $\Gamma_2 = (M_2/M_1)\Gamma_1 \approx 0.03\, M_2$. This scaling is what would be expected for the reference model SSM [31].

For illustrative purposes, the invariant mass distribution of $W^{\pm}$ pairs in the process $pp \to W^+W^+ + X$ in the SM (solid black curve) and for the $Z'_{\rm SSM}$ model at two vaues of the Z-Z' mixing angle at the LHC with $\sqrt{s} = 14$ TeV is shown in Fig. 1. The $W^{\pm}$-pair invariant mass distribution $(d\sigma/dM)$ is calculated with the same parton distribution functions and event selection criterion as those used in Ref. [32]. Also, the bin size ΔM of the diboson invariant mass is depicted for comparison with the Z' width. For numerical computations, we take $\Delta M = 0.03M$. The W bosons are kept on-shell and their subsequent decays are not included in the crosss sections represented in Fig. 1. Here, we assumed that the invariant mass distribution of the cross section can be reconstructed from the decay products of the W^+W^-. Fig. 1 shows that at the LHC with integrated luminosity $\mathcal{L}_{\rm int} = 100$ fb^{-1} the expected number of W^+W^- background events within a mass bin ΔM is of the order of a few events while the resonant yield at $\phi = 10^{-3}$ is $N_{Z'} \sim 100$.

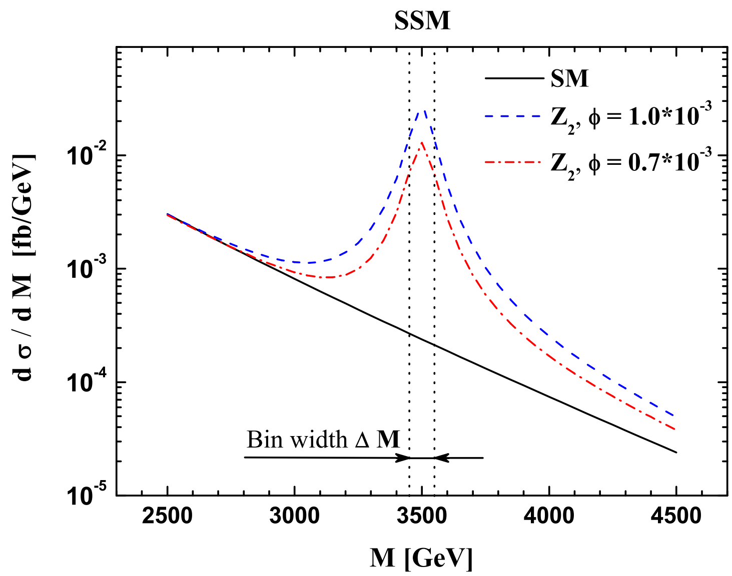

Figure 1: Invariant mass distribution of $W^{\pm}$ pairs in $pp \to W^+W^- + X$ in the SM (solid curve) and for the $Z'_{\rm SSM}$ model ($M_{Z'} = 3.5$ TeV) with Z-Z' mixing angle of $\phi = 10^{-3}$ (dashed line) and $\phi = 0.7 \cdot 10^{-3}$ (dash-dotted line) at the LHC with $\sqrt{s} = 14$ TeV.

4 Constraints on Z'

We focus on the WW production via intermediate Z' and subsequent purely leptonic decay of on-shell W's, that will be probed at LHC:

$$pp \to WW + X \to l\nu l'\nu' + X \quad (l, l' = e \text{ or } \mu), \tag{15}$$

and, we follow the analysis given in [27, 33, 34], to evaluate the main backgrounds and possible cuts to enhance the Z' signal to background ratio.

In our analysis, we denote by $N_{\rm SM}$ and $N_{Z'}$ the numbers of 'background' and 'signal' events, and we adopt the criterion $N_{Z'} = 2\sqrt{N_{\rm SM}}$ or 3 events, whichever is larger, as the minimum signal for reach at the 95% C.L. [4]. Here, the Z' signal can be determined as

$$N_{Z'} = \mathcal{L}_{\rm int} \times \sigma^{Z'} \times P^{\rm EW}_{\rm surv} \times A \times \epsilon^{\ell}, \tag{16}$$

with

$$\sigma^{Z'} = \sigma(pp \to Z') \times {\rm Br}(Z' \to W^+W^- \to l\nu l'\nu'). \tag{17}$$

In Eq. (16), $\mathcal{L}_{\rm int}$ is the time-integrated luminosity, and $A\times\epsilon^\ell$ is the product of the overall acceptance times the lepton detection and reconstruction efficiencies where A represents the kinematic and geometric acceptance from the total phase space to the fiducial phase space governed by Eqs. (9) and (10), while ϵ^ℓ represents detector effects such as lepton trigger and identification efficiencies. The overall acceptance times the lepton efficiency is $W^\pm$ invariant mass dependent and, for simplicity, we take that to be 0.5. The SM background reads:

$$N_{\rm SM} = \mathcal{L}_{\rm int}\left(\sigma^{\rm EW}_{\rm SM}\, P^{\rm EW}_{\rm surv} + \sigma^{t\bar{t}}_{\rm SM}\, P^{\rm QCD}_{\rm surv}\right) A\,\epsilon^\ell \approx \mathcal{L}_{\rm int}\,\sigma^{\rm EW}_{\rm SM}\, P^{\rm EW}_{\rm surv}\, A\,\epsilon^\ell, \qquad (18)$$

where $\sigma^{\rm EW}_{\rm SM}$ is determined by Eqs. (11) and (13) taking into account solely the SM contribution. Also, in the latter expression for $N_{\rm SM}$ we take into account that for heavy $M_{Z'}$, $\sigma^{\rm EW}_{\rm SM} \gg \sigma^{t\bar{t}}_{\rm SM}$ as was shown in [33].

We depict in Fig. 2 the region in parameter space to which the LHC will be able to constrain Z-Z' mixing for $\mathcal{L}_{\rm int} = 100$ fb^{-1}.

In particular, the discovery reach on the Z-Z' mixing and M_2 mass for $Z'_{\rm SSM}$ obtained from the process $pp \to WW + X \to l\nu l'\nu' + X$ $(l, l' = e$ or $\mu)$ at the LHC with $\sqrt{s} = 14$ TeV and $\mathcal{L}_{\rm int} = 100$ fb^{-1} are depicted by the two solid lines. The form of these bounds is governed by the criterion of $N_{Z'} = 3$ and the quadratic dependence of the resonant cross section on the Z-Z' mixing angle. Also, current limits on M_2 for $Z'_{\rm SSM}$ derived from the Drell–Yan (l^+l^-) process at the LHC (8 TeV) (horizontal solid line) as well as those expected from the future experiments at the LHC with 14 TeV (horizontal dotted line) are shown. The combined allowed area in the (ϕ, M_2) plane obtained from the Drell–Yan and $W^\pm$ pair production processes is shown as a hatched region. In addition, present limits on the Z-Z' mixing angle obtained from electroweak precision data analysis [10] labelled as 'EW data' are displayed (these have a weak mass dependence which we have not attempted to draw). For comparison, the corresponding limits obtained from $W^\pm$ pair production at the ILC with polarized beams and for two options of energy and time-integrated luminosity (0.5 (1) TeV and 0.5 (1) ab^{-1}, respectively) are also presented [17]. Fig. 2 show that the LHC is able to not only significantly improve the current limits on the Z-Z' mixing angle, but in several cases, also allow more stringent bounds than those expected from future experiments on the WW channel at the electron–positron collider ILC [11].

In Table 1, we collect our limits on the Z' parameters for the models listed in Section II. Also shown in Table 1 are the current limits on vari-

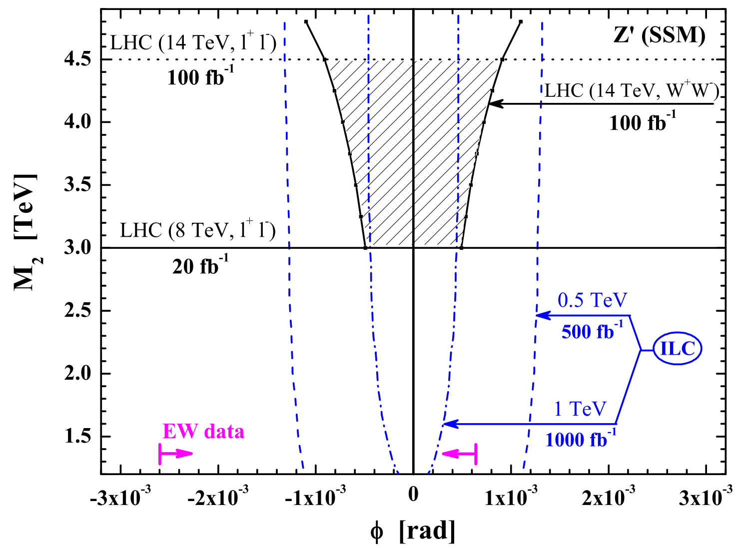

Figure 2: Reach (at 95 %C.L.) on Z-Z' mixing and M_2 mass for $Z'_{\rm SSM}$ obtained from the inclusive process $pp \to WW \to l\nu l'\nu'$ $(l, l' = e$ or $\mu)$ at the LHC (solid lines). The allowed domain in ϕ and M_2 is the hatched one. Current limits on M_2 for $Z'_{\rm SSM}$ derived from the Drell–Yan (l^+l^-) process at the LHC (8 TeV) (horizontal solid line) as well as 'typical' mass limits expected at the LHC (14 TeV) (horizontal dotted line) are shown. Limits on the Z-Z' mixing angle from electroweak precision data are displayed, and those expected from $W^\pm$ pair production at the ILC with polarized beams.

ous Z' boson masses from the LEP2 and Tevatron from studies of diboson W^+W^- pair production. The limits on ϕ and M_2 at the Tevatron assume that no decay channels into exotic fermions or superpartners are open to the Z'. Otherwise, the limits would be moderately weaker. LEP2 constrains virtual and Z-Z' boson mixing effects by the angular distribution of W bosons. Table 1 shows that the limits on ϕ from the EW precision data are generally competitive with and in many cases stronger than those from the colliders, except for the ILC (1 TeV) and LHC (14 TeV) that possess high potential to improve substantially the current bounds on the Z-Z' mixing angle. We stress that these limits are highly complementary.

If a new Z' boson exists in the mass range $\sim$ 3–4.5 TeV, its discovery is possible in the Drell–Yan channel. Moreover, the detection of the $Z' \to W^+W^-$ mode is eminently possible and gives valuable information

Table 1: Reach on the Z-Z' mixing angle ϕ at 95% C.L. in different processes and experiments.

collider, process	$\|\phi\|\times$	Z'_χ $\|\phi\|$	Z'_ψ $\|\phi\|$	Z'_η $\|\phi\|$	Z'_{SSM} $\|\phi\|$	$M_{Z'}$ (TeV)
LEP2 [11], $e^+e^- \to W^+W^-$	10^{-2}	6	15	50	7	≥ 1
Tevatron [12], $p\bar{p} \to W^+W^- + X$	10^{-2}	–	–	–	2	0.4–0.9
electroweak data [10]	10^{-3}	1.6	1.8	4.7	2.6	–
ILC (0.5 TeV) [17], $e^+e^- \to W^+W^-$	10^{-3}	1.5	2.3	1.6	1.2	≥ 3
ILC (1.0 TeV) [17], $e^+e^- \to W^+W^-$	10^{-3}	0.4	0.6	0.5	0.3	≥ 3
LHC (8 TeV), $pp \to W^+W^- \to l\nu l'\nu'$	10^{-3}	–	–	–	5.2	3
LHC (14 TeV), $pp \to W^+W^- \to l\nu l'\nu'$	10^{-4}	4–8	3–6	3–6	5–9	3–4.5

on the Z-Z' mixing. It might be the only mode other than the dileptonic one, $Z' \to l^+l^-$, that is accessible. Our results demonstrate that it might be possible to detect a new heavy Z' boson from the totally leptonic or semileptonic WW channels at the LHC. The LHC at nominal energy and integrated luminosity provides the best opportunity of studying a new heavy Z' through its WW decay mode and creates the possibility of measuring (or constraining) the Z-Z' mixing, thus providing insight into the pattern of symmetry breaking.

Acknowledgments

This research has been partially supported by the Abdus Salam ICTP (TRIL Programme), the Collaborative Research Center SFB676/1-2006 of the DFG at the Department of Physics of the University of Hamburg and the Belarusian Republican Foundation for Fundamental Research.

References

[1] J. Beringer *et. al.* [PDG], Phys. Rev. D **86**, 010001 (2012).

[2] J. L. Hewett and T. G. Rizzo, Phys. Rept. **183**, 193 (1989).

[3] P. Langacker, Rev. Mod. Phys. **81**, 1199-1228 (2009).

[4] A. Leike, Phys. Rept. **317**, 143-250 (1999).

[5] A. Gulov and V. Skalozub, Int. J. Mod. Phys. A **25**, 5787 (2010).

[6] S. Chatrchyan *et al.* [CMS Collab.], Phys. Lett. B **720**, 63 (2013).

[7] G. Aad *et al.* [ATLAS Collab.], JHEP **1211**, 138 (2012).

[8] G. Aad *et al.* [ATLAS Collab.], arXiv:1405.4123 [hep-ex].

[9] [CMS Collab.], CMS-PAS-EXO-12-061.

[10] J. Erler, P. Langacker, S. Munir, E. Rojas, JHEP **0908**, 017 (2009).

[11] V. V. Andreev and A. A. Pankov, Phys. Atom. Nucl. **75**, 76 (2012).

[12] T. Aaltonen *et al.* [CDF Collab.], Phys. Rev. Lett. **104**, 241801 (2010).

[13] S. Schael *et al.* [ALEPH and DELPHI and L3 and OPAL and SLD and LEP Electroweak Working Group and SLD Electroweak Group and SLD Heavy Flavour Group Collab.], Phys. Rept. **427**, 257 (2006).

[14] S. Godfrey and T. Martin, arXiv:1309.1688 [hep-ph].

[15] M. Dittmar, A. Nicollerat, A. Djouadi, Phys. Lett. B **583**, 111 (2004).

[16] T. G. Rizzo, [hep-ph/0610104].

[17] V. V. Andreev, G. Moortgat-Pick, P. Osland, A. A. Pankov and N. Paver, Eur. Phys. J. C **72**, 2147 (2012).

[18] B. Ananthanarayan, M. Patra, P. Poulose, JHEP **1102**, 043 (2011).

[19] V. M. Abazov *et al.* [D0 Collab.], Phys. Rev. Lett. **107**, 011801 (2011).

[20] G. Aad *et al.* [ATLAS Collab.], Phys. Rev. D **87**, 112006 (2013).

[21] G. Aad *et al.* [ATLAS Collab.], Phys. Lett. B **718**, 860 (2013).

[22] J. M. Campbell and R. K. Ellis, Phys. Rev. D **60**, 113006 (1999).

[23] J. M. Campbell, R. K. Ellis and C. Williams, JHEP **1107**, 018 (2011).

[24] N. Agarwal, V. Ravindran, V. K. Tiwari and A. Tripathi, Phys. Rev. D **82**, 036001 (2010).

[25] Y. -M. Bai, L. Guo, X. -Z. Li, W. -G. Ma and R. -Y. Zhang, Phys. Rev. D **85**, 016008 (2012).

[26] J. Pumplin, D. R. Stump, J. Huston, H. L. Lai, P. Nadolsky and W. K. Tung, JHEP **0207**, 012 (2002).

[27] V. V. Andreev, P. Osland and A. A. Pankov, Phys. Rev. D **90**, no. 5, 055025 (2014).

[28] P. Osland, A. Pankov, N. Paver, A. Tsytrinov, Phys. Rev. D **78**, 035008 (2008).

[29] [ATLAS Collab.], CERN-LHCC-99-14, CERN-LHCC-99-15.

[30] A. A. Pankov and N. Paver, Phys. Rev. D **48**, 63 (1993).

[31] D. Benchekroun, C. Driouichi and A. Hoummada, Eur. Phys. J. direct C **3**, N3 (2001).

[32] N. Agarwal, V. Ravindran, V. K. Tiwari and A. Tripathi, Phys. Lett. B **690**, 390 (2010).

[33] A. Alves, O. J. P. Eboli, D. Goncalves, M. C. Gonzalez-Garcia and J. K. Mizukoshi, Phys. Rev. D **80**, 073011 (2009).

[34] O. J. P. Eboli, C. S. Fong, J. Gonzalez-Fraile and M. C. Gonzalez-Garcia, Phys. Rev. D **83**, 095014 (2011).